Nerve Endings With Structural Characteristics of Mechanoreceptors in the Human Scleral Spur

Ernst R. Tamm, Cassandra Flügel, Fritz H. Stefani, and Elke Lütjen-Drecoll*

Purpose. The innervation of the scleral spur region was investigated to learn whether mechanoreceptors are present in this region.

Methods. Serial tangential sections and whole-mount preparations of the scleral spur region of 18 human eyes of different ages were investigated with electronmicroscopic and immunohistochemical methods. For immunohistochemistry antibodies against neurofilament-proteins, synaptophysin, substance P (SP), calcitonin gene-related peptide (CGRP), vasoactive intestinal polypeptide (VIP), neuropeptide Y (NPY), tyrosine-hydroxylase, dopamine-β-hydroxylase, and acetylcholinesterase were used.

Results. Club- or bulb-shaped nerve endings with a diameter of 5 μm to 25 μm were identified in the scleral spur region throughout the whole circumference of the eyes. The terminals derive from myelinated axons with a diameter of approximately 3 μm and stain with antibodies against neurofilament-proteins and synaptophysin but do not stain for tyrosine-hydroxylase, dopamine-β-hydroxylase, acetylcholinesterase, NPY, VIP, SP, or CGRP. Electronmicroscopically, the endings contain abundant neurofilaments, granular and agranular vesicles of different sizes, numerous mitochondria, and lysosome-like lamellated structures. The endings are incompletely ensheathed by Schwann cells. Those areas of the cell membrane of the endings that are not covered by Schwann cells are in intimate contact with the fibrillar connective tissue elements of the scleral spur.

Conclusion. These structural features are highly characteristic for mechanoreceptive nerve endings in other tissues of the human body. The authors therefore hypothesize that the club- or bulb-shaped nerve endings in the human scleral spur are afferent mechanoreceptors that measure stress or strain in the connective tissue elements of the scleral spur. Such changes might be induced by ciliary muscle contraction and/or by changes in intraocular pressure. Invest Ophthalmol Vis Sci. 1994;35:1157–1166.

The inner layers of the mammalian eye are supplied by sensory nerves that originate from the trigeminal ganglion. The majority of these trigeminal fibers consist of unmyelinated fibers of the C-type.[1–4] Immunohistochemical studies indicate that the terminals of the fibers may contain certain neuropeptides, such as substance P or calcitonin gene-related peptide, that are known to play an important role in the irritative response of the eye[5–7] It is not known whether some of the ocular sensory nerves function as visceral mechanoreceptors. In general, visceral mechanoreceptors are stretch-receptors that are able to measure stress or strain in their surrounding connective tissue elements[8–10] The afferent terminals of mechanoreceptors show several structural characteristics, such as a high content of mitochondria, granular, and agranular vesicles of different sizes, lysosome-like lamellated bodies, numerous neurofilaments, and a close contact of their cell membrane with connective tissue fibrils[11–15] In the chamber angle, visceral mechanoreceptors might be important to monitor ciliary muscle tone and/or variations in intraocular pressure (IOP). The morphologic search for such specialized receptors in the chamber angle, and in other regions of the primate eye as well, has been without clear result.[2,16] In the present study,

*From the Department of Anatomy II, University of Erlangen-Nürnberg, Erlangen, and the *Eye Hospital of the University of Munich, Munich, Germany.*
Presented in part at the annual meeting of the Association for Research in Vision and Ophthalmology, Sarasota, Florida, May 2–7, 1993.
Supported by grants from the Deutsche Forschungsgemeinschaft (Ta 115/5-1) and the Academy for Science and Literature, Mainz, Germany.
Submitted for publication March 16, 1993; revised September 21, 1993; accepted September 22, 1993.
Proprietary interest category: N.
Reprint requests: Dr. Ernst R. Tamm, Department of Anatomy II, University of Erlangen-Nürnberg, Universitätsstrasse 19, 91054 Erlangen, Germany.

we investigated the scleral spur region in human eyes with ultrastructural and immunocytochemical methods. We report on a group of nerve endings, not previously described, that share typical structural characteristics with mechanoreceptive nerve endings in visceral organs such as the carotid sinus,[17-21] aortic arch,[22] respiratory system,[23,24], atrial endocardium,[25] and esophagus.[26,27] We therefore suggest that the human scleral spur region contains mechanoreceptors. Although their functional role is not yet clarified, the possibility exists that these sensory receptors are involved in the regulation of IOP.

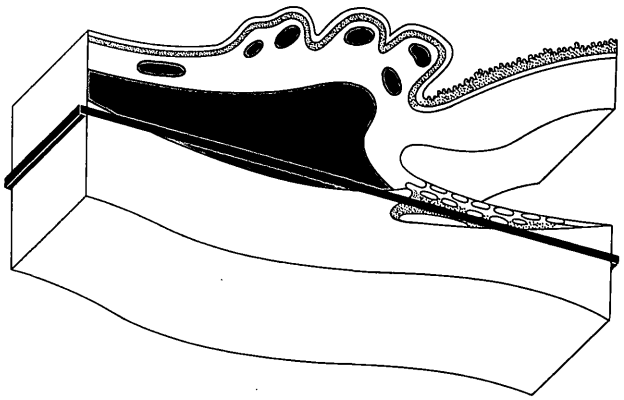

FIGURE 1. Schematic drawing of the anterior segment of the eye showing the sectional plane of the tangential sections through the scleral spur region.

MATERIALS AND METHODS

Ten pairs of human eyes (age range, 28 to 87 years) obtained after autopsy and eight eyes enucleated because of posterior choroidal melanoma (age range, 33 to 81 years) were investigated. The melanoma eyes were obtained from the Eye Hospital of the University of Munich, Germany. None of the donors had any history of abnormality in the chamber angle. Methods for securing human tissue were humane, included proper consent and approval, and complied with the Declaration of Helsinki.

The eyes were cut equatorially behind the ora serrata, and the anterior segment was dissected in quadrants. From each quadrant, wedge-shaped pieces containing trabecular meshwork and the anterior ciliary muscle were cut. The specimens were immersed in Zamboni's[28] or Ito's solution[29] for 24 hours at 4°C. All specimens from autopsy eyes were placed in fixative within 4 hours after death; specimens from two pairs of these autopsy eyes (ages 33 and 68 years) were fixed within 20 minutes after death.

Electron Microscopy

Specimens fixed in Ito's solution were processed for electron microscopy. After fixation with 1% osmium tetroxide, the specimens were dehydrated with graded alcohols and embedded in Epon (Roth, Karlsruhe, Germany). Serial meridional, frontal, and tangential semithin and ultrathin sections were cut on a microtome. Figure 1 shows the sectional plane of the tangential sections. Semithin sections were stained with Richardson's stain.[30] Ultrathin sections were treated with lead citrate and uranyl acetate and viewed using a Zeiss EM 902 microscope (Zeiss, Oberkochen, Germany).

IMMUNOHISTOCHEMISTRY

Specimens fixed in Zamboni's solution were washed for 24 hours in phosphate-buffered saline (PSB) and quick frozen in isopentane, precooled with liquid nitrogen, or embedded in paraffin. Meridional and serial tangential (Fig. 1) cryostat sections were cut at a thickness of 20 or 50 μm, and paraffin sections were cut at a thickness of 5 μm. The sections were placed on slides covered with 0.1% poly-L-lysine and preincubated for 45 minutes in Blotto's dry milk solution.[31] After preincubation, the sections were incubated overnight at room temperature with the primary antibodies. Final dilutions of all antibodies contained 0.3% Triton X-100 and 2% bovine serum albumin. For demonstration of neurofilament proteins, monoclonal antibodies from Dakopatts (Hamburg, Germany, clone 2F11, 1:100) and Boehringer (Mannheim, Germany, clone RT97, 1:25)[32] were used. For synaptophysin, a monoclonal antibody from Dakopatts (clone SY38)[33] was applied to the slides at a dilution of 1:10. Demonstration of tyrosine-hydroxylase, dopamine-β-hydroxylase, and substance P was performed using polyclonal rabbit antibodies from Eugene Tech (Ramsey, NJ, 1:200). Acetylcholinesterase was visualized with rabbit antibodies from Chemicon (Temecula, CA, 1:200). Vasoactive intestinal polypeptide and calcitonin gene-related peptide were stained with polyclonal rabbit antibodies from Medscand Diagnostics (Lund, Sweden, 1:1000), whereas neuropeptide Y was visualized with polyclonal rabbit antibodies from Amersham Buchler (Braunschweig, Germany, 1:80). After overnight incubation, the sections were washed in PBS, reacted for 1 hour with biotinylated secondary antibodies (Amersham), washed again, and covered with streptavidin-FITC (Dakopatts).

Double-staining experiments were performed by incubating sections with a combination of synaptophysin antibodies and polyclonal rabbit antibodies against neurofilament proteins (Sigma, St. Louis, MO). Binding of the monoclonal antibody was visualized using the biotin-streptavidin-FITC system as described above, and the rabbit antiserum was stained with a Texas red conjugated anti-rabbit IgG (Amersham).

After washing in PBS, the sections were mounted in Entellan (Merck, Darmstadt, Germany) containing

1,4-Diazabicyclo [2,2,2] octan (DABCO, Merck)[34] and viewed with a Leitz Aristoplan microscope (Ernst Leitz GmbH, Wetzlar, Germany). Some of the sections were viewed with a BioRad MRC 600 confocal laser scanning microscope (BioRad Microscience Ltd., Hemel Hempstead, UK). A Kodak T-max 400 film was used for photography.

For whole-mount staining, the anterior meridional ciliary muscle portion, scleral spur, and trabecular meshwork were dissected and separated from other ocular structures. The tissues were passed through graded alcohols to xylene (30 minutes each step) and returned through alcohols to xylene[35] The free floating tissue preparations were incubated in primary antibody for 24 hours at 4°C, followed by incubation with biotinylated antibodies against mouse Ig (Amersham) and a streptAB-Complex (Amersham). After development in diaminobenzidine hydrogen peroxide solution, the tissues were mounted on microscope slides.

Staining with antibodies against the different neuropeptides visualized varicose terminals with the typical spatial distribution, as described for each of these peptides in the chamber angle of human eyes.[5,6] Negative control experiments were performed using either PBS or mouse or rabbit pre-immune serum substituted for the primary antibody.

In the eyes of four donors (ages 28, 33, 68, and 81 years), the number of club- or bulb-shaped terminals positively stained for neurofilament proteins and the distance between them were quantified. Whole mounts of the temporal sector of the scleral spur with 10 mm circumferential length were viewed with a light microscope using a magnification of × 20 and analyzed with an image processing and analysis system (Quantimed 500, Leica Cambridge Ltd, Cambridge, UK).

RESULTS

Light Microscopy

Neurofilament Proteins. Antibodies against neurofilament proteins label myelinated nerve fibers as well as larger unmyelinated axons. Thus, immunostaining for neurofilament proteins, applied to serial sections and whole-mount preparations containing the anterior meridional ciliary muscle, scleral spur, and trabecular meshwork, visualizes the architecture of all larger axons in this area. Both monoclonal and polyclonal antibodies against neurofilament proteins give similar results.

Numerous axons are positively stained for neurofilament proteins in the meridional portion of the ciliary muscle, near its insertion to the scleral spur. The axons run meridionally, e.g., parallel to the ciliary muscle bundles. In the interstitial or intermuscular spaces between the muscle bundles, solitary myelinated axons with a diameter of 2 to 3.5 μm predominate. Most of these axons branch and give rise to thinner unmyelinated axons that enter the muscle bundles and terminate between the individual muscle cells. Some of the myelinated axons do not branch in the muscle but continue toward the anterior insertion of the muscle at the scleral spur. Having passed the anterior insertion of the ciliary muscle, these axons turn circumferentially into the scleral spur to run parallel to the elastic and collagenous fibers of the spur. Thus, the axons give rise to a loose network of circumferentially oriented myelinated axons in the scleral spur. Myelinated axons that do not pass through the ciliary muscle but run in a meridional direction in the supraciliary space (e.g., the uveoscleral interface) also turn circumferentially at the spur and join the network of circumferential spur axons. Most of these spur axons are observed at the inner aspect of the scleral spur. Some of the axons pass forward to the uveal meshwork, others branch and provide both spur and meshwork. In places, the myelinated spur axons lose their myelin sheath, branch profusely, and terminate by expanding to club- or bulb-like structures with a range in size of 5 to 10 μm (Figs. 2, 3). In eyes of humans younger than 40 years of age, these structures are regularly observed in all quadrants of the circumference. Quantitative analysis in the eyes of two young donors (ages 28 and 32 years), using whole-mounts of a temporal sector of the scleral spur with 10 mm circumferential length, shows an average distance between the nerve endings of 1.11 ± 0.4 mm and 1.32 ± 0,33 mm (Table 1). Most of these endings are observed at the inner aspect of the spur (Fig. 3). Some of these club-shaped endings, however, are also found deeper in the spur tissue, near the anterior insertion of the ciliary muscle, or in the posterior parts of the uveal trabecular meshwork.

In the eyes of humans older than 70 years of age, the club-shaped terminals are larger, with a range in size of 20 to 25 μm (Figs. 2B, 2C). In addition, these endings are more frequently observed in older rather than in younger donors. Quantitative analysis in the eyes of two old donors (ages 68 and 81 years) shows an average distance between nerve endings of 0.3 ± 0.23 mm and 0.44 ± 0.22 (Table 1). Similar to the eyes of young humans, the terminals are regularly observed in all quadrants of the circumference.

Synaptophysin. In the ciliary muscle, antibodies against synaptophysin intensely label the visceroefferent nerve endings. Each individual smooth muscle cell is surrounded by approximately 10 to 15 of these nerve endings, which measure 0.5 to 1 μm in diameter (Fig. 5A). In the scleral spur and the trabecular meshwork, positive staining of a considerable number of

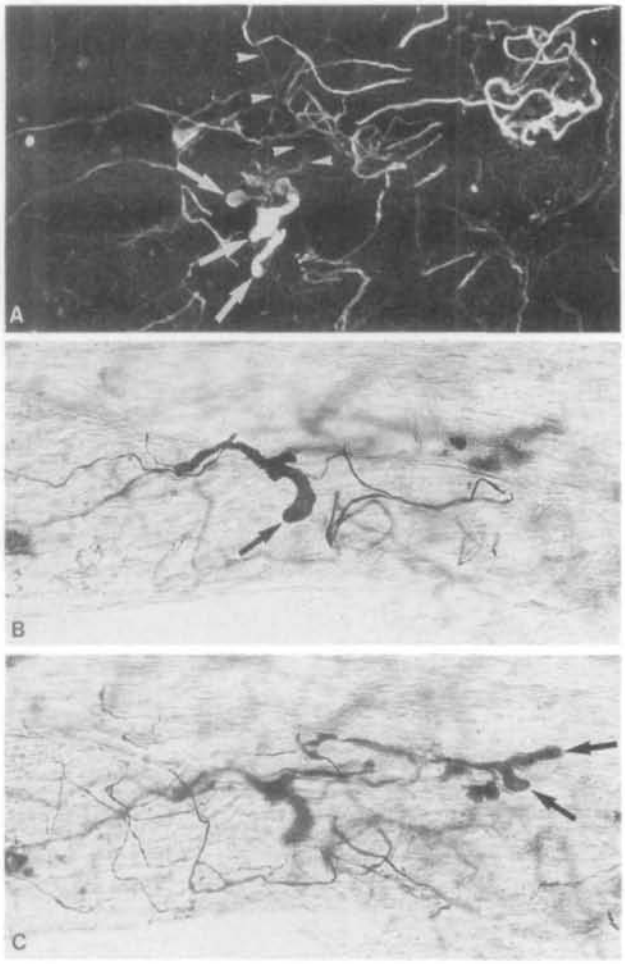

FIGURE 2. (A) Tangential cryostat section (Fig. 1 shows sectional plane) (B, C) and whole-mount preparation of a sector of the scleral spur with 0.5 mm circumferential length immunostained with antibodies against neurofilament proteins. The orientation of the micrographs is similar to that in Figure 4. The anterior insertion of the ciliary muscle is situated beyond the top of the individual micrographs, the trabecular meshwork beyond the bottom. (A) 50 μm tangential section of the scleral spur of a 32-year-old donor viewed with confocal laser scanning microscope. Numerous positively stained axons are seen in the scleral spur. One of these axons (arrowheads) branches profusely and terminates by expanding to club- or bulb-like structures (arrows, immunofluorescence, overlay image of 22 serial sections of 2 μm thickness, × 150). (B, C) Whole mount of the scleral spur of a 67-year-old donor. Both lightmicrographs were taken from the same specimen in different planes of focus. Two club- or bulb-shaped terminals are seen (arrows). In the eyes of older donors, the club-shaped nerve terminals are larger, ranging in size from 20 to 25 μm, and are more numerous than in the eyes of younger donors (immunoperoxidase, × 150).

varicose terminals, which derive from unmyelinated axons, is observed. In contrast, the myelinated axons in this area do not stain for synaptophysin. However, the club- or bulb-shaped terminals, which originate

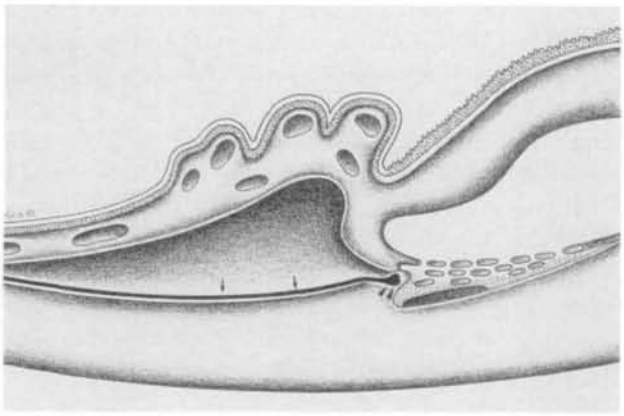

FIGURE 3. Schematic drawing of the anterior segment of the eye showing the localization of the club- or bulb-shaped nerve terminals in the scleral spur. Myelinated axons pass through the ciliary muscle or through the supraciliary space (arrows). In the scleral spur, the axons lose their myelin sheath, branch profusely, and terminate by expanding to club- or bulb-like structures (arrowheads).

from these axons, express intense positive immunoreactivity for synaptophysin (Figs. 4, 5A).

Double staining with antibodies against both neurofilament and synaptophysin show that staining for neurofilament proteins is more confined to the central area of these endings, whereas staining for synaptophysin predominates in their peripheral parts (Figs. 5B, 5C). The varicose axons of the unmyelinated axons in scleral spur and trabecular meshwork stain only for synaptophysin but not for neurofilament. The same is true for the visceroefferent terminals around the ciliary muscle cells.

The enlarged, club-shaped endings in the eyes of older donors show intense immunoreactivity for neurofilament proteins, whereas staining for synaptophysin is usually weaker than it is in the eyes of young donors. In addition, in the older eyes some of the endings stain for neurofilament proteins but not for synaptophysin.

TABLE 1. Quantitative Evaluation of the Club-Shaped Terminals in the Scleral Spur Region

Age (Yr)	*No. of Terminals*	*Distance Between Terminals (mm) (Mean ± SD)*
28	9	1.11 ± 0.4
33	8	1.32 ± 0.35
68	31	0.30 ± 0.23
81	21	0.44 ± 0.22

In the eyes of four human donors, whole-mount preparations of the temporal sector of the scleral spur region were immunostained for neurofilament proteins. The specimens had a total circumferential length of 10 mm and were analyzed with an image processing and analysis system.

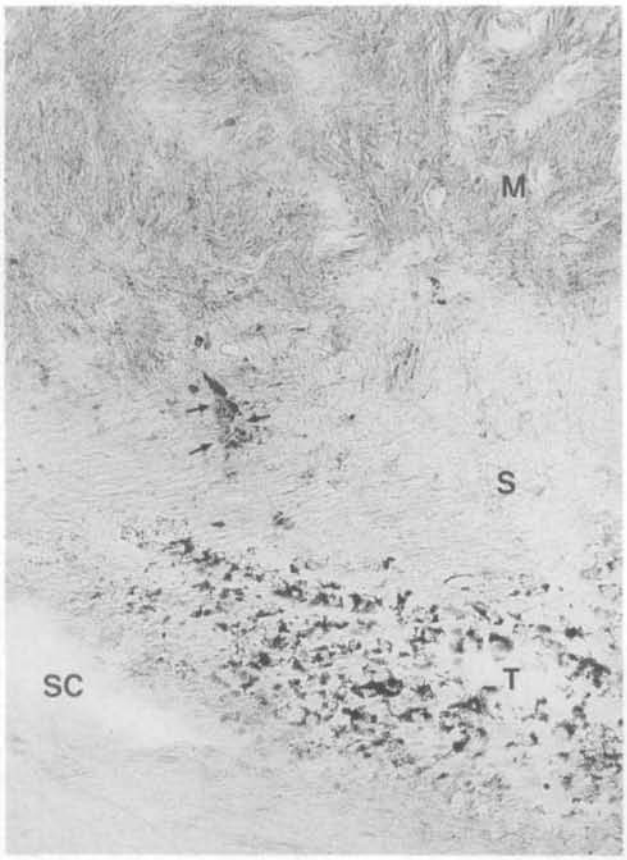

FIGURE 4. Five micrometer tangential paraffin section (Fig. 1 shows sectional plane) through the scleral spur region of a 68-year-old donor immunostained for synaptophysin (immunoperoxidase counterstained with Mayer's hematoxylin, × 100). A club- or bulb-shaped terminal (arrows) in the scleral spur (S) is positively stained. At the posterior aspect of the scleral spur, the ciliary muscle (M) bundles are seen in region of their insertion to the scleral spur. Anteriorly, the scleral spur is continuous with the trabecular meshwork (T), which is heavily pigmented in this specimen. SC, Schlemms canal.

Electron Microscopy

The scleral spur does not show the extreme dense innervation of the ciliary muscle. As previously described,[36] most of the nerve terminals in this region are found in close proximity to the scleral spur cells. These terminals have a diameter of 0.5 to 1 μm and contain predominantly small agranular (30 to 60 nm) and large granular (65 to 100 nm) vesicles embedded in an electron-lucent cytoplasm. In addition, nerve terminals are observed that differ markedly in size and structure from those scleral spur cell nerve endings (Fig. 6). These terminals are identical with the club- or bulb-shaped terminals visualized by immunohistochemistry. The terminals are ultrastructurally characterized by their large content of mitochondria interspersed between numerous 8 to 10 nm thick neurofilaments (Figs. 6, 7). In addition, there are numerous granular and agranular vesicles that vary considerably in size (30 to 150 nm) (Figs. 6, 7). Between mitochondria and vesicles, lysosome-like, concentric, osmiophilic lamellae resembling myelin figures are often observed (Figs. 7, 8). Close to the cell membrane, all these structures are embedded in a fine filamentous matrix.

The surface of the club-shaped terminals is partly ensheathed by flat processes of Schwann cells. Nonetheless, large parts of the cell membranes of the terminals are still exposed directly to the extracellular connective tissue elements. In these areas, the endings remain covered by a basal lamina continuous with the basal lamina of the surrounding Schwann cells. In addition, the elastic fibers in the scleral spur are in close proximity to the terminals in these regions. The fibers show the characteristic ultrastructure of the elastic

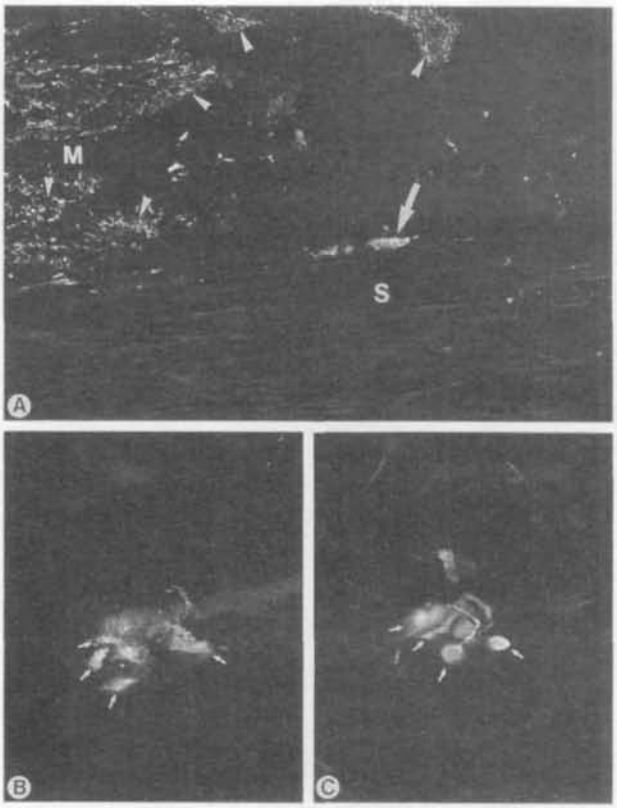

FIGURE 5. Immunofluorescence of the human scleral spur region (donor age, 56 years). (**A**) Frontal cryostat section through anterior meridional ciliary muscle portion (M) and scleral spur (S) stained for synaptophysin. In the ciliary muscle, visceroefferent nerve terminals (arrowheads) are positively stained. In addition, positive immunofluorescence is seen in a club-shaped terminal (arrows) located at the inner aspect of the scleral spur (× 150). (**B**, **C**) Double immunostaining for synaptophysin (**B**) and neurofilament proteins (**C**) of a tangential cryostat section (sectional plane similar to Figs. 1, 2, 4) through the scleral spur. Club-shaped terminals (arrows) are positively labeled with both antibodies (× 500).

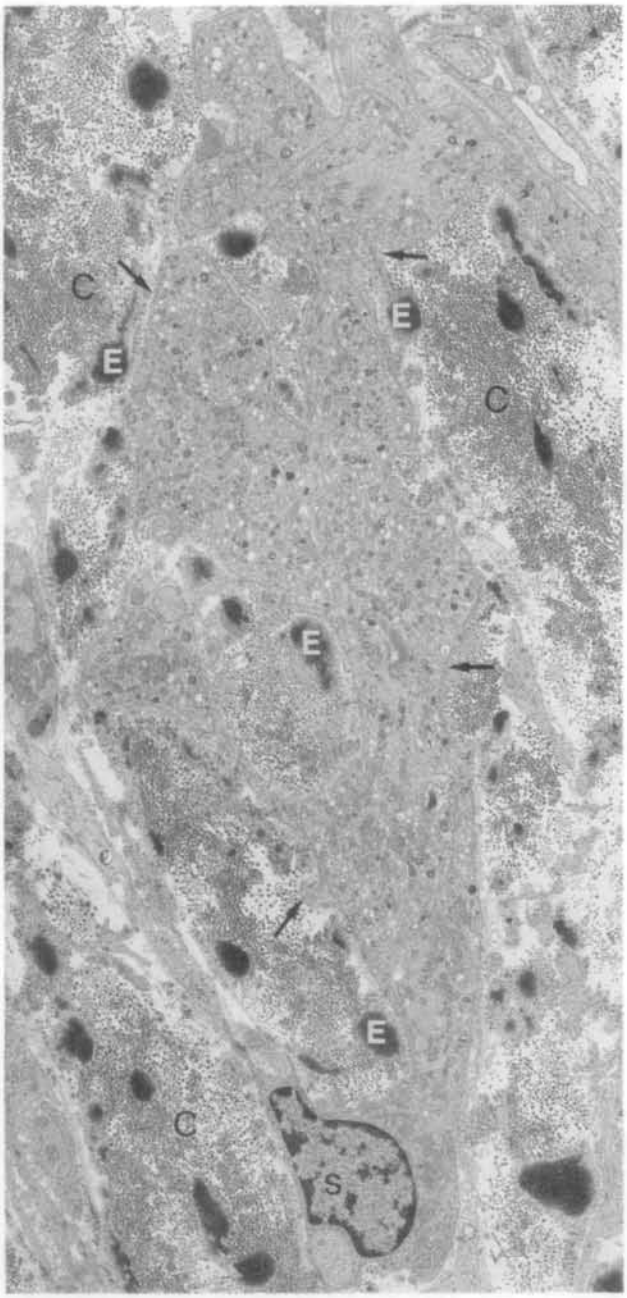

FIGURE 6. Electronmicrograph of a club-shaped terminal in the scleral spur (donor age, 38 years). The terminal has a length of approximately 25 μm and is densely surrounded by collagen (C) and elastic fibers (E). The surface of the terminal is partly ensheathed by flat processes of Schwann cells (S). Nonetheless, large parts of the cell membrane are still exposed directly to the extracellular fibrils (arrows, × 6300).

fibers in the chamber angle tissues[37,38] because they comprise an electron-dense amorphous central core and a sheath consisting of microfibrils and cross-banded material with a periodicity of 50 to 60 nm. The 50 to 60 nm cross-banded sheath material of the elastic fibers merges with the basal lamina and contacts the cell membrane of the endings directly (Figs. 7, 8, 9). In some areas of contact with the cross-banded sheath material, the cell membrane of the terminals has specialized electron-dense areas (Fig. 10). Some of the terminals form protrusions that surround larger parts of elastic fibers (Figs. 8, 9). Serial ultrathin sections confirm that the club-shaped endings derive from myelinated axons with a diameter of about 3 to 3.5 μm. The axons lose their myelin sheath and form distinc-

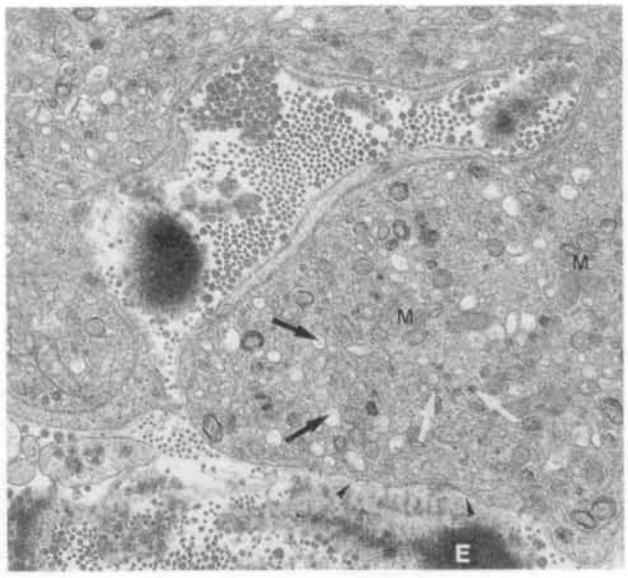

FIGURE 7. Higher magnification of Figure 3 (× 14,000). The cytoplasm of the terminal contains numerous mitochondria (M) as well as agranular (black arrows) and granular vesicles (white arrows) that are embedded in a filamentous matrix. The 50 to 60 nm cross-banded sheath material of an elastic fiber (E) merges with the basal lamina of the terminal and contacts the cell membrane (arrowheads).

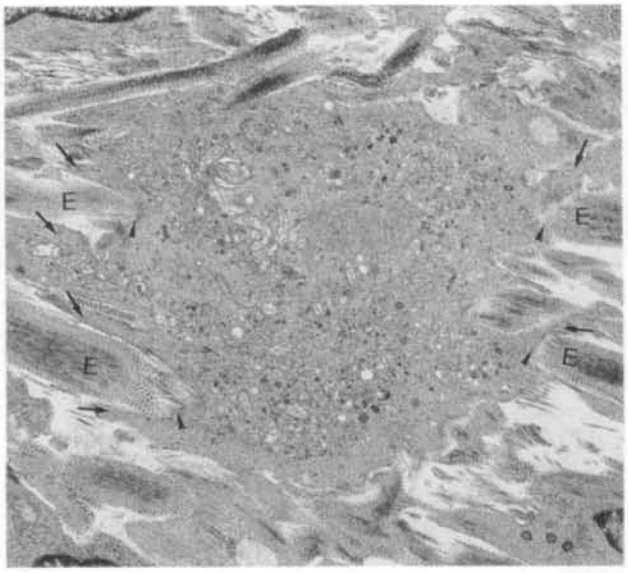

FIGURE 8. Tangential section of a scleral spur terminal (electronmigrograph × 5,000; donor age, 56 years). The terminal is embedded in a meshwork of numerous, circularly oriented elastic fibers (E) that are in close contact with the cell membrane of the terminal (arrowheads). In addition, the terminal forms protrusions that surround larger parts of the elastic fibers (arrows).

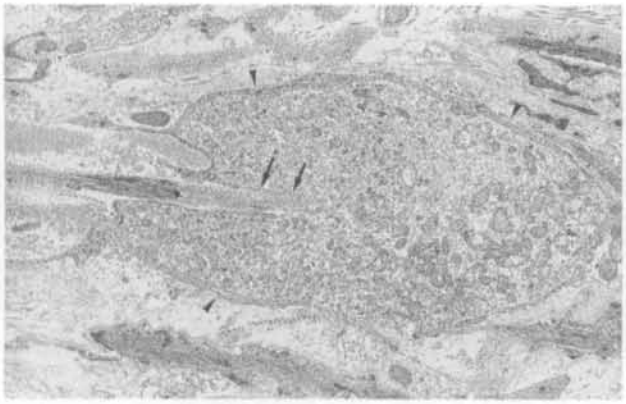

FIGURE 9. Meridional section of a club-shaped terminal in the scleral spur (donor age, 34 years). The terminal contains numerous mitochondria, vesicles, and a filamentous matrix. An elastic fiber (asterisk) is wrapped by cytoplasmic protrusions of the terminal. The terminal is ensheathed by flat processes of terminal Schwan cells (arrowheads). Nevertheless, in regions of contact with the the elastic fiber, the cell membrane of the terminal is not covered by such Schwann cells but is in direct contact with the cross-banded sheath material of the elastic fiber (arrows, electronmicrograph × 5,800).

tive half nodes of Ranvier (Fig. 11). Before expanding to the typical terminals, the unmyelinated preterminal axons continue their course in the scleral spur tissue for several micrometers.

Tyrosine-Hydroxylase, Dopamine-β-Hydroxylase, Acetylcholinesterase, SP, CGRP, VIP, NPY

Antibodies against tyrosine-hydroxylase and dopamine-β-hydroxylase stain some presumably adrenergic varicose terminals in ciliary muscle, scleral spur, and trabecular meshwork, whereas staining for acetylcholinesterase is strictly confined to the ciliary muscle bundles. Staining with antibodies against the different neuropeptides visualizes varicose terminals with the typical spatial distribution, as described for each of these peptides in the chamber angle of human eyes.[5,6]

FIGURE 10. High-power electronmicrograph of a club-shaped terminal (× 33,000). In some areas of contact with the 50 to 60 nm cross-banded sheath material of the elastic fibers (E), the cell membrane of the terminal (asterisk) has specialized electron-dense areas (arrow).

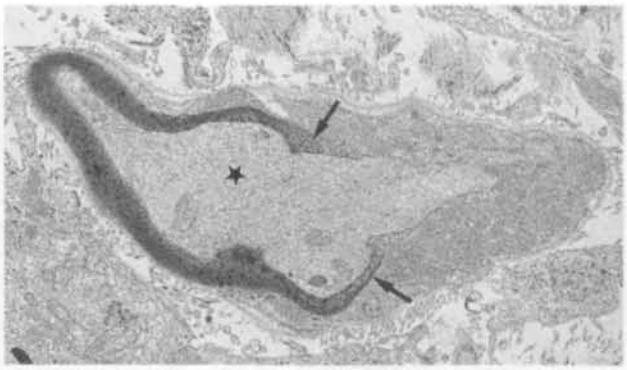

FIGURE 11. The club-shaped terminals derive from myelinated axons with a diameter of 3 to 3.5 μm. The axons (asterisk) lose their myelin sheath (arrows) and form distinctive half nodes of Ranvier (electronmicrograph, × 7,000).

The club-shaped nerve endings are not stained with any of these antibodies.

DISCUSSION

The presence of nerve fibers in the anterior chamber angle of monkey and human eyes is well documented.[6,39] In the trabecular meshwork of both species, most of the nerve fibers were reported to be unmyelinated, whereas in the scleral spur myelinated axons also were observed.[40,41]

Our study confirms the presence of myelinated axons in the scleral spur and provides evidence that a considerable number of these axons terminate as distinctive club- or bulb-shaped structures. These terminals might be identical to nervous aggregates described in earlier studies by means of silver-impregnation techniques and discussed as baroreceptors.[42,43]

Our results show that in common with the visceroefferent nerve endings of the ciliary muscle cells and the terminals of the unmyelinated varicose axons in scleral spur and trabecular meshwork, the club-shaped terminals stain positively for synaptophysin. Synaptophysin is a transmembranous glycoprotein specifically localized to synaptic vesicles and the vesicular structures of neuroendocrine cells.[44] The immunoreactivity for synaptophysin is not confined just to efferent nerve endings but is also observed in afferent terminals.[45] It has been suggested that the small agranular vesicles present in such afferent terminals are most probably stained.[45]

In contrast to the ciliary muscle terminals and the terminals of the unmyelinated axons, the club-shaped endings show intense immunoreactivity with antibodies against neurofilament proteins. It is generally agreed upon that neurofilaments predominate in myelinated axons.[46] It has been demonstrated in rat sensory ganglia that one of the antibodies (RT97) used in the present study specifically stains large neurons of the A type, which have a fast conducting myelinated axon.[47,48]

Ultrastructurally, the club-shaped nerve endings show characteristic features that are regarded as typical for the receptive areas of afferent nerve endings in skin, tendons, and joint capsules,[11,12,15,49,50] or in various visceral organs.[17-19,22,27] These common characteristics are as follows: a high content of mitochondria; granular and agranular vesicles of different sizes; lysosome-like lamellated bodies; numerous neurofilaments; and a fine filamentous matrix in region of the receptive cell membrane, the so-called "receptor matrix."[13,14] We therefore suggest that the club-shaped nerve endings in the human scleral spur are terminals of primary afferent neurons. Indeed, degeneration studies have shown that 20% of the axons in the scleral spur of cynomolgus monkeys have a sensory origin from the trigeminal ganglion.[41] So far, however, ultrastructural studies have failed to demonstrate distinctive sensory nerve endings in the human chamber angle comparable to those described in our study.

Characteristically, the club-shaped terminals in the scleral spur region are in close contact with the extracellular fibrillar material of their surrounding connective tissue. It is primarily the numerous elastic fibers in the spur that are in close proximity to the cell membrane of the endings. In general, such contacts between extracellular fibrils and sensory nerve terminals are characteristic of mechanoreceptors. They have been described for the mechanoreceptive nerve endings of the Golgi tendon organ,[51,52] the encapsulated Ruffini corpuscles of the skin,[53] and for visceral mechanoreceptors such as the branched lanceolate or ruffini-like corpuscles of the respiratory system,[23,24] the dura mater encephali,[54] the periodontal ligament,[55-58] and vascular structures such as the carotid sinus,[17,18] the aortic arch,[22] or the atrial endocardium.[25]

It seems probable that the club-shaped spur terminals serve a mechanoreceptive function. In general, mechanoreceptors are in contact with accessory structures that transfer a mechanical disturbance in the local environment to a mechanosensitive region of the receptor.[59] The mechanisms of mechanotransduction in visceral mechanoreceptors, which measure stretch and distention of the organs of the gastrointestinal, respiratory, urogenital, and vascular system, are not fully understood. The current hypothesis is that stretch in surrounding connective tissue elements that are in close contact with the cell membrane of the receptor influences stretch-sensitive ion channels in the membrane.[8,10,59] The mechanical linkage between channel and membrane is thought to be provided by cytoskeletal strings that pull the membrane open when the membrane is stretched. Such cytoskeletal coupling may explain the prominent occurrence of microfilaments in the transducing region of this type of mechanoreceptor.[59] Mechanoreceptors or stretch-receptors in the scleral spur should measure stress or strain in the connective tissue elements of the spur. Because these factors are surely influenced by changes in ciliary muscle tone, the nerve endings might represent proprioreceptive "tendon organs" of the ciliary muscle. In addition, contraction of the scleral spur cells, which form microtendon-like connections with the elastic fibers of the spur,[36] might modulate the tension of the fibers. On the other hand, the scleral spur, with its circumferentially arranged collagen and elastic fibers,[60] is the innermost part of the outer coat of the eye, the sclera. Changes in intraocular pressure exert influence on stress or strain of the sclera and probably also on stress of the scleral spur. Thus, mechanoreceptors that measure stretch of the scleral spur might also have a baroreceptive function. Interestingly, most visceral receptors that measure distention of the gastrointestinal and urogenital tracts and vascular system are directly or indirectly associated with smooth muscles. Contraction of smooth muscle can modulate the excitability or may lead to excitation of visceral receptors by changing visceral compliance.[8] Physiological studies suggest that baroreceptive nerve terminals might exist in the eye because sensory discharges in the ciliary nerves related to IOP changes have been observed.[61-65] Belmonte et al[64] suggested that the ciliary nerves in the cat eye contain afferent fibers that respond tonically within the normal range of IOP and originate from specific, slowly adapting mechanoreceptors sensitive to variations in IOP.

Morphologically, such mechanoreceptors have not been described in mammalian eyes. An exception are the eyes of such aquatic mammals as whales and dolphins.[66,67] In these animals, lamellated paccinian corpuscles are present in the chamber angle and may represent specialized structures important to adapt to changes between aquatic and atmospheric environments.[39]

The putative mechanoreceptive nerve endings in the human scleral spur show structural changes with age that include an increase in diameter. Interestingly, silver impregnation studies by Wolter,[68] Vrabec,[69] and Valu,[70] described an axonal swelling of nerve fibers in the chamber angle as typical senile change of this tissue, which was more pronounced in glaucomatous eyes.[68] It might be that these studies also visualized an age- or disease-related enlargement of the scleral spur terminals.

In summary, we hypothesize that mechanoreceptive nerve endings are present in the human scleral spur. The physiological role of these structures remains to be clarified.

Key Words

mechanoreceptor, sensory nerve terminal, scleral spur, chamber angle, human eye

Acknowledgments

The authors thank Angelika Hauser and Simone Klein for expert assistance with immunohistochemistry and electron-microscopy, and Marco Göβwein and Anette Gach for prepa-

ration of the photographs and drawings. They also thank BioRad Microsciences Ltd., Hemel Hempstead, UK, for the use of the confocal laser scanning microscope to examine specimens.

References

1. Holland MG, von Sallmann L, Collins EM. A study of the innervation of the chamber angle: II: The origin of trabecular axons revealed by degeneration. *Am J Ophthalmol.* 1957;44:206–221.
2. Bergmannson JPG. The ophthalmic innervation of the uvea in monkeys. *Exp Eye Res.* 1977;24:225–240.
3. Ten Tuscher MPM, Klooster J, Van der Want JJL, Lamers WPMA, Vrensen GFJM. The allocation of nerve fibers to the anterior segment and peripheral ganglia of rats: I: The sensory innervation. *Brain Res.* 1989;494:95–104.
4. Beckers HJM, Klooster J, Vrensen GFJM, Lamers WPMA. Ultrastructural identification of trigeminal nerve endings in the rat cornea and iris. *Invest Opthalmol Vis Sci.* 1992;33:1979–1986.
5. Stone RA, Kuwayama Y, Laties AM. Regulatory peptides in the eye. *Experientia.* 1987;43:791–800.
6. Stone RA, Kuwayama Y. The nervous system and intraocular pressure. In: Ritch R, Shields MB, Krupin T, eds. *The glaucomas.* St. Louis: CV Mosby; 1989:257–279.
7. Bill A. The 1990 Endre Balazs Lecture: Effects of some neuropeptides on the uvea. *Exp Eye Res.* 1991;53:3–11.
8. Jänig W, Morrison JFB. Functional properties of spinal visceral afferents supplying abdominal and pelvic organs, with special emphasis on visceral nociception. In: Cervero F, Morrison JFB, eds. *Progress in Brain Reserach.* Vol. 67. Amsterdam: Elsevier; 1986:87–114.
9. Widdicombe JG. Sensory innervation of the lungs and airways. In: Cervero F, Morrison JFB, eds. *Progress in Brain Research.* Vol. 67. Amsterdam: Elsevier; 1986:49–64.
10. Kumada M, Terui N, Kuwaki T. Arterial baroreceptor reflex: Its central and peripheral neural mechanisms. *Prog Neurobiol.* 1990;35:331–361.
11. Halata Z. The mechanoreceptors of the mammalian skin: Ultrastructure and morphological classification. *Adv Anat Embryol Cell Biol.* 1975;50:1–77.
12. Chouchkov C. Cutaneous receptors. *Adv Anat Embryol Cell Biol.* 1978;54:1–61.
13. Andres KH. Morphological criteria for the differentiation of mechanoreceptors in vertebrates. In: Schwartzkopff J, ed. *Symposium Mechanorezeption, Abhdlg. Rhein. Westf. Akad. Wiss. 53.* Opladen: Westdeutscher Verlag; 1974:135–152.
14. Andres KH, von Düring M. Morphology of cutaneous receptors. In: Iggo A, ed. *Handbook of sensory physiology.* Berlin, Heidelberg, New York: Springer Verlag; 1973:3–28.
15. Iggo A, Andres KH. Morphology of cutaneous receptors. *Annu Rev Neurosci.* 1982;5:1–31.
16. Ruskell GL. Innervation of the anterior segment of the eye. In: Lütjen-Drecoll E, ed. *Basic Aspects of Glaucoma Research.* Stuttgart: Schattauer Verlag; 1982:49–66.
17. Rees PM. Observations on the fine structure and distribution of presumptive baroreceptor nerves at the carotid sinus. *J Comp Neurol.* 1967;131:517–548.
18. Böck P, Gorgas K. Fine structure of baroreceptor terminals in the carotid sinus of guinea pigs and mice. *Cell Tissue Res.* 1976;170:95–112.
19. Knoche H, Addicks K. Electron microscopic studies of the pressoreceptor fields of the carotid sinus of the dog. *Cell Tissue Res.* 1976;173:77–94.
20. Knoche H, Walther-Wenke G, Addicks K. Die Feinstruktur der barorezeptorischen Nervenendigungen in der Wand des Sinus caroticus der Katze. *Acta Anat.* 1977;97:403–418. (In German.)
21. Knoche H, Wiesner-Menzel L, Addicks K. Ultrastructure of baroreceptors in the carotid sinus of the rabbit. *Acta Anat.* 1980;106:63–83.
22. Krauhs JM. Structure of rat aortic baroreceptors and their relationship to connective tissue. *J Neurocytol.* 1979;8:401–404.
23. von Düring M, Andres KH, Iravani J. The fine structure of the pulmonary stretch receptor in the rat. *Z Anat Entwickl-Gesch.* 1974;143:215–222.
24. von Düring M, Andres KH. Structure and functional anatomy of visceroreceptors in the mammalian respiratory system. In: Hamann W, Iggo A, eds. *Progress in Brain Research.* Vol. 74. Amsterdam: Elsevier; 1988:139–154.
25. Tranum-Jensen J. The ultrastructure of the sensory end-organs (baroreceptors) in the atrial endocardium of young mini-pigs. *J Anat.* 1975;119:255–275.
26. Neuhuber WL. Sensory vagal innervation of the rat esophagus and cardia: A light and electron microscopic anterograde tracing study. *J Auton Nerv Syst.* 1987;20:243–255.
27. Neuhuber WL, Clerc N. Afferent innervation of the esophagus in cat and rat. In: Zenker W, Neuhuber WL, eds. *The Primary Afferent Neuron.* New York: Plenum; 1990:93–107.
28. Stefanini M, de Martino C, Zamboni C. Fixation of ejaculated spermatozoa for electron microscopy. *Neuroscience.* 1967;216:173–174.
29. Ito S, Karnovsky MJ. Formaldehyde-glutaraldehyde fixatives containing trinitro compounds. *J Cell Biol.* 1968;39:168A–169A.
30. Richardson KC, Jarret L, Finke H. Embedding in epoxy resins for ultrathin sectioning in electron microscopy. *Stain Technol.* 1960;35:313–323.
31. Duhamel RC, Johnson DA. Use of nonfat dry milk to block nonspecific nuclear and membrane staining by avidin conjugates. *J Histochem Cytochem.* 1985;33:711–714.
32. Wood JN, Anderton BH. Monoclonal antibodies to mammalian neurofilaments. *Biosci Rep.* 1981;1:263–268.
33. Wiedenmann B, Franke WW. Identification and localization of synaptophysin, an integral membrane glycoprotein of Mr 38000 characteristic of presynaptic vesicles. *Cell.* 1985;41:1017–1028.
34. Johnson GD, Davidson RS, McNamee KC, Rusel G, Goodwin D, Holborow EJ. Fading of immunofluorescence during microscopy: A study of the phenomenon and its remedy. *J Immunol Methods.* 1982;55:231–242.
35. Costa M, Furness JB, Solcia E. Immunohistochemical localization of polypeptides in peripheral autonomic

nerves using whole mount preparations. *Histochemistry.* 1080;65:157–165.
36. Tamm E, Flügel C, Stefani FH, Rohen JW. Contractile cells in the human scleral spur. *Exp Eye Res.* 1992;54:531–543.
37. Vegge T, Ringvold A. The ultrastructure of the extracellular components of the trabecular meshwork in the human eye. *Z Zellforsch.* 1971;11:361–376.
38. Rohen JW, Futa R, Lütjen-Drecoll E. The fine structure of the cribriform meshwork in normal and glaucomatous eyes as seen in tangential sections. *Invest Opthalmol Vis Sci.* 1981;21:574–585.
39. Stone RA, Laties AM. Neuroanatomy and neuroendocrinology of the chamber-angle. In: Krieglstein GK, ed. *Glaucoma Update III.* Berlin: Springer Verlag; 1987:1–16.
40. Feeney L. Ultrastructure of the nerves in the human trabecular region. *Invest Opthalmol Vis Sci.* 1962; 1:462–473.
41. Ruskell GL. The source of nerve fibres of the trabeculae and adjacent structures in monkey eyes. *Exp Eye Res.* 1976;23:449–459.
42. Kurus E. Über ein Ganglienzellsystem der menschlichen Aderhaut. *Klin Mbl Augenheilk.* 1955;127:198–206. (In German.)
43. Castro-Correira J. Studies on the innervation of the uveal tract. *Ophthalmologica.* 1967;154:497–520.
44. Wiedenmann B, Huttner WB. Synaptophysin and chromogranins/secretogranins: Widespread constituents of distinct types of neuroendocrine vesicles and new tools in tumor diagnostics. *Virchows Archiv B Cell Pathol.* 1989;58:95–121.
45. De Camilli P, Vitadello M, Canevini MP, Zanoni R, Jahn R, Gorio A. The synaptic vesicle proteins synapsin I and synaptophysin (protein p38) are concentrated both in efferent and afferent nerve endings of the skeletal muscle. *J Neurosci.* 1988;8:1625–1631.
46. Lawson SN, Harper AA, Harper EI, Garson JA, Anderton BH. A monoclonal antibody against neurofilament protein specifically labels a subpopulation of rat sensory neurons. *J Comp Neurol.* 1984;228:263–272.
47. McCarthy PW, Lawson SN. Cell type and conduction velocity of rat primary sensory neurons with substance P-like immunoreactivity. *Neuroscience.* 1989;28:745–753.
48. McCarthy PW, Lawson SN. Cell type and conduction velocity of rat primary sensory neurons with calcitonin gene-related peptide-like immunoreactivity. *Neuroscience.* 1990;34:623–632.
49. Halata Z, Rettig T, Schulze W. The ultrastructure of sensory nerve endings in the human knee joint capsule. *Anat Embryol.* 1985;172:265–275.
50. Halata Z. The ultrastructure of the sensory nerve endings in the articular capsule of the domestic cat (Ruffini corpuscles and Pacinian corpuscles). *J Anat.* 1977;124:717–729.
51. Schoultz TW, Swett JE. The fine structure of the Golgi tendon organ. *J Neurocytol.* 1972;1:1–26.
52. Schoultz TW, Swett JE. Ultrastructural organization of the sensory fibers innervating the Golgi tendon organ. *Anat Rec.* 1974;179:147–162.
53. Chambers MR, von Düring M, Iggo A. The structure and function of the slowly adapting type II mechanoreceptor in hairy skin. *Q J Exp Physiol.* 1972;57:417–445.
54. Andres KH, von Düring M, Muszynski K, Schmidt RF. Nerve fibers and their terminals of the dura mater encephali of the rat. *Anat Embryol.* 1987;175:289–301.
55. Everts V, Beertsen W, Van den Hoof A. Fine structure of an end organ in the periodontal ligament of the mouse incisor. *Anat Rec.* 1977;189:73–90.
56. Maeda T, Sato O, Kobayashi S, Iwanaga T, Fujita T. The ultrastructure of ruffini endings in the periodontal ligament of rat incisors with special reference to the terminal Schwann cells (K-cells). *Anat Rec.* 1989;223:95–103.
57. Kannari K, Sato O, Maeda T, Iwanaga T, Fujita T. A possible mechanism of mechanoreception in ruffini endings in the periodontal ligament of hamster incisors. *J Comp Neurol.* 1991;313:368–376.
58. Sato O, Maeda T, Kannari K, Kawahara I, Iwanaga T, Takano Y. Innervation of the periodontal-ligament in the dog with special reference to the morphology of ruffini endings. *Arch Histol Cytol.* 1992;55:21–30.
59. Detwiler PB. Sensory transduction. In: Patton HD, Fuchs AF, Hille B, Scher AM, Steiner R, eds. *Textbook of Physiology: Excitable Cells and Neurophysiology.* Vol. 1. Philadelphia: WB Saunders; 1989:98–129.
60. Moses RA, Grodzki WJ, Starcher BC, Galione MJ. Elastin content of the scleral spur, trabecular mesh and sclera. *Invest Opthalmol Vis Sci.* 1978;17:817–818.
61. von Sallmann L, Fuortes MGF, Macri FJ, Grimes P. Study of afferent electric impulses induced by intraocular pressure changes. *Am J Ophthalmol.* 1958;45: 211–220.
62. Lele PP, Grimes P. The role of neural mechanisms in the regulation of intraocular pressure in the cat. *Exp Neurol.* 1960;2:199–220.
63. Perkins ES. Sensory mechanisms and intraocular pressure. *Exp Eye Res.* 1961;1:160–167.
64. Belmonte C, Simon J, Gallego A. Effects of intraocular pressure changes on the afferent activity of ciliary nerves. *Exp Eye Res.* 1971;12:342–355.
65. Zuazo A, Ibanez J, Belmonte C. Sensory nerve responses elicited by experimental ocular hypertension. *Exp Eye Res.* 1986;43:759–769.
66. Vrabec F. Encapsulated sensory corpuscles in the sclerocorneal boundary tissues of the killer whale *Orcinus orca L. Acta Anat.* 1972;81:23–29.
67. Wickham MG. Irido-corneal angle of mammalian eyes: Comparative morphology of encapsulated corpuscles in odontocete cetaceans. *Cell Tissue Res.* 1980;210:501–515.
68. Wolter JR. Neuropathology of the trabeculum in open-angle glaucoma. *Arch Ophthalmol.* 1959;62:99–111.
69. Vrabec F. On the development and senile changes of the innervation of the trabecular meshwork in humans. In: Rohen JW, ed. *The structure of the eye.* Vol. 2. Stuttgart: Schattauer Verlag; 1965:215–222.
70. Valu L. Über die Innervation des Uvea-Trabekel-Systems. *Graefe's Arch Clin Exp Ophthalmol.* 1962;164: 496–502. (In German.)